

Toward Atomic-Resolution Quantum Measurements with Coherently Shaped Free Electrons

Ron Ruimy^{1,*}, Alexey Gorlach^{1,*}, Chen Mechel¹, Nicholas Rivera,² and Ido Kaminer^{1,†}

¹*Solid State Institute, Technion-Israel Institute of Technology, Haifa 32000, Israel*

²*Department of Physics, Massachusetts Institute of Technology, Cambridge, Massachusetts 02139, USA*



(Received 31 October 2020; accepted 30 March 2021; published 11 June 2021)

Free electrons provide a powerful tool for probing material properties at atomic resolution. Recent advances in ultrafast electron microscopy enable the manipulation of free-electron wave functions using laser pulses. It would be of great importance if one could combine the spatial resolution of electron microscopes with the ability of laser pulses to probe coherent phenomena in quantum systems. To this end, we propose a novel concept that leverages free electrons that are coherently shaped by laser pulses to measure quantum coherence in materials. We develop the quantum theory of interactions between shaped electrons and arbitrary qubit states in materials, and show how the postinteraction electron energy spectrum enables measuring the qubit state (on the Bloch sphere) and the decoherence or relaxation times (T_2/T_1). Finally, we describe how such electrons can detect and quantify superradiance from multiple qubits. Our scheme can be implemented in ultrafast transmission electron microscopes (UTEM), opening the way toward the full characterization of the state of quantum systems at atomic resolution.

DOI: [10.1103/PhysRevLett.126.233403](https://doi.org/10.1103/PhysRevLett.126.233403)

Introduction.—Electron microscopy and spectroscopy are powerful methods to extract information about quantum emitters such as atoms, molecules, and solids [1]. State-of-the-art techniques include cathodoluminescence (CL) [1–3] and electron energy-loss spectroscopy (EELS) [1,4,5], which measure excitation energies, band gaps, and the local density of photonic states (LDOS) [6] with high spatial resolution. However, much information cannot normally be extracted: for example, the quantum state of material excitations, decoherence times (T_2), and generally any information associated with off-diagonal density-matrix elements of quantum systems. Looking beyond electron microscopy, it is of fundamental interest to determine the quantum information that is exchanged in the interaction of free electrons and quantum emitters. For brevity, we refer to the quantum systems as “qubits,” since we focus on a single material excitation that corresponds to a fixed electron transition.

In the case of qubits in the optical range, their quantum state and decoherence times can be analyzed using laser-based coherent control [7] and pump-probe laser experiments [8–13]. Yet, the probing of individual qubits in optical experiments has limited spatial resolution set by the optical wavelength: measuring an individual emitter, rather than an ensemble, requires a *dilute* sample. Dilute ensembles render the acquisition of sufficient signals a substantial challenge. Frequently, high densities of qubits are intrinsic to their fabrication and important for applications [14–16], such as semiconductor quantum dot (SQD) devices for quantum science and technology [17–19] or applications involving qubit-qubit interactions for quantum gates and quantum information processing [20–22].

The ability to distinguish between homogeneous and inhomogeneous broadening in emitters is highly desired [23]. It is especially important to have ways to measure the decoherence rates of individual emitters (T_2) and differentiate them from the ensemble collective decoherence rate (T_2^*) that relates to inhomogeneous broadening. Such a distinction is also of technological relevance, e.g., in high color-contrast displays [24]. Usually, in *dense* emitter ensembles, T_2 can only be measured through indirect techniques such as spin echo, giving the ensemble average of many different T_2 values [25,26]. These challenges motivate the use of free electrons as highly localized probes that can quantify the quantum properties of individual qubits.

Here we propose a scheme to access coherent quantum information of qubits using coherently shaped free electrons. We show how controlling the incident-shaped electron enables measurement of the qubit state and the extraction of the longitudinal (T_1) and transverse (T_2) relaxation rates of the qubit. Such measurements can be performed using a pump-probe scheme in which the pump is a laser pulse and the probe is the electron. We develop a theory to describe the interaction of electrons with a two-level system characterized by a transition dipole moment, relevant to many types of excitations in different systems (e.g., defect centers and direct band-gap transitions). The results are stronger for larger dipoles, as with excitons in 2D semiconductor heterostructures [27], perovskites [28–30], and Rydberg state atoms [31,32].

Our work is motivated by advances in ultrafast electron spectroscopy and microscopy [1], especially photon-induced

nearfield electron microscopy (PINEM) [33–36], which demonstrated how femtosecond-pulsed lasers can shape free-electron wave functions transversely [37] and longitudinally [38,39] (i.e., coherently modulated electrons). These advances reveal various new applications in condensed matter physics, quantum technology, and even nuclear physics. Interestingly, the PINEM theory was recently extended to capture the interaction of free electrons with quantized light [40–42] revealing new applications such as free-electron entanglement [40].

We propose a method that takes advantage of shaped electrons to extract the coherent state and decoherence rates of qubits. We quantify how this concept can be implemented in electron microscopes using EELS and CL and how it can enhance their signals. These enhancements agree with some of the semiclassical predictions presented in Ref. [43], based on the classical modulation of free electrons. We show how the quantum description goes beyond this theory and provides capabilities that cannot be modeled semiclassically.

Apart from T_2 , our scheme can also measure T_1 , which provides information about the LDOS. Importantly, T_1 can also be extracted at high spatial resolution using recent advances in time-resolved CL [1,2]. In comparison, our scheme could provide a femtosecond (and eventually attosecond) temporal resolution. Such short timescales enable probing phenomena such as superradiance [44,45]. Altogether, our schemes could lead to a full toolbox of high-resolution capabilities for reading and writing arbitrary states of qubits in materials.

Quantum interaction of qubits and free electrons.—We can model the electron-qubit interaction by the Hamiltonian

$$H = -i\hbar v \partial_z + \frac{\hbar\omega_0}{2} \sigma_z + \frac{e}{4\pi\epsilon_0} \cdot \frac{(\mathbf{d}_\perp \cdot \mathbf{r}_\perp + d_\parallel z) \sigma_+ + (\mathbf{d}_\perp^* \cdot \mathbf{r}_\perp + d_\parallel^* z) \sigma_-}{(r_\perp^2 + z^2)^{3/2}}, \quad (1)$$

where the first two terms describe the Hamiltonians of the electron and the qubit. The average velocity of the electron wave packet is v . The qubit has an energy separation of $\hbar\omega_0$; σ_\pm , σ_z are Pauli matrices. The third term in Eq. (1) describes the interaction with the transition dipole moment $\mathbf{d} = g|er\rangle|e$, with components $\mathbf{d}_\parallel = \hat{z}d_z$ and $\mathbf{d}_\perp = \hat{x}d_x + \hat{y}d_y$. The distance between the center of the electron wave packet and the center of the qubit (the impact parameter) is r_\perp ; the vacuum permittivity is ϵ_0 . The full derivation of Eq. (1) is presented in the Supplemental Material [46], Sec. II (SM-II, which contains Ref. [47]).

The approximations behind Eq. (1) are (I) Paraxial approximation for the electron is valid since the energy of

the electron is much larger than that of the excitation. (II) External decoherence channels by other material excitations [48], such as Bremsstrahlung radiation [49] and characteristic x ray [50], occur at probabilities much smaller than unity. Thus, the reduced density matrix of the electron and the qubit (for the excitation of interest) will be the same as if the external channels are not considered at all. See SM-I [46] for further discussion.

The scattering matrix can be found from the Magnus expansion [51] as

$$S = e^{-i(g\sigma^+ b + g^* b^+ \sigma^- + \kappa\sigma_z)}. \quad (2)$$

Here, the operators b and b^+ are momentum translation operators for the electron and $b = e^{i\omega_0 z/v}$ [52] (for sufficiently fast electrons, they equivalently describe energy translation); g and κ are the interaction parameters.

The interaction strength g is typically small ($|g| \ll 1$) and then can be approximated as

$$g = \frac{ed_x \omega_0 K_1(\frac{\omega_0 r_\perp}{v})}{2\pi\epsilon_0 \hbar v^2} + i \frac{ed_z \omega_0 K_0(\frac{\omega_0 r_\perp}{v})}{2\pi\epsilon_0 \hbar v^2}, \quad (3)$$

where $K_0(x)$ and $K_1(x)$ are modified Bessel functions of the second kind; SM-III [46] describes the general derivation for relativistic electron-qubit interactions, showing corrections to g (that do not change the concepts shown below). The interaction constant κ in Eq. (2) under the approximation of $|g| \ll 1$ can be neglected:

$$S = e^{-i(g\sigma^+ b + g^* b^+ \sigma^-)} = \cos|g| - i \cdot \sin|g| (e^{i\phi_g} \sigma_+ b + e^{-i\phi_g} \sigma_- b^+), \quad (4)$$

where ϕ_g is the phase of the interaction constant g .

Consider a qubit prepared (e.g., by an optical pulse) in a coherent superposition $|\psi\rangle = a_1|g\rangle + a_2|e\rangle$. The qubit undergoes decoherence and relaxation [Fig. 1(c)], leading to a density matrix at time τ (SM-IV [46], which contains Ref. [53]):

$$\rho_a(\tau) = \begin{pmatrix} 1 - |a_2|^2 e^{-\tau/T_1} & e^{-\tau/T_2} a_1 a_2^* e^{i\omega_0 \tau} \\ e^{-\tau/T_2} a_1^* a_2 e^{-i\omega_0 \tau} & |a_2|^2 e^{-\tau/T_1} \end{pmatrix}. \quad (5)$$

A shaped electron interacts with this qubit. The density matrix after the electron-qubit interaction is $\rho_f = S^+ \rho_i S$, where $\rho_i = \rho_a \otimes \rho_e$ and ρ_e are the initial density matrices of the joint system and electron, respectively. We measure the EELS of the postinteraction electron, which provides the diagonal of the electron density matrix after the interaction $\text{tr}_{\text{qubit}} \rho_f$ [Fig. 1(d)]. This measurement contains information about the off-diagonal terms of Eq. (5) if the initial electron is a superposition of several energies that differ by the qubit energy gap $\hbar\omega_0$. Such

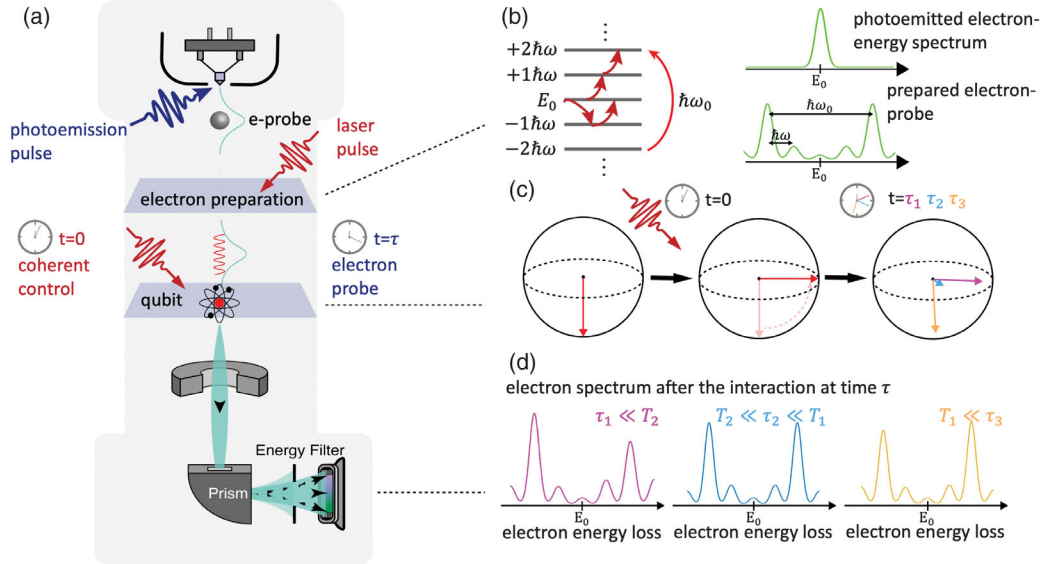


FIG. 1. Coherently shaped free electrons as high-resolution probes of coherence in quantum systems. (a) An ultrafast transmission electron microscope where (b) electrons are coherently shaped by a PINEM interaction, creating a superposition of energies spaced by integer multiples of the driving laser frequency ω , chosen so the gap between a certain pair of electron energies matches the qubit energy $\hbar\omega_0$. (c) The qubit is excited to $1/\sqrt{2}|g\rangle + i/\sqrt{2}|e\rangle$ and interacts with the electron after time delay τ . (d) The postinteraction electron is measured as a function of τ , using electron energy loss spectroscopy (EELS). This scheme enables measuring different qubit properties, e.g., extracting T_2 from the asymmetry of the spectrum.

shaped electrons can be generated via PINEM [Figs. 1(a) and (b)].

Measurement of relaxation and decoherence times.—We first consider the interaction of a conventional electron that was not pre-shaped by the laser (i.e., “unshaped electron,” or zero-loss peak). The EELS features of unshaped electrons interacting with a qubit are proportional to $|g|^2$. For example, a pump-probe scheme with unshaped electrons can measure T_1 (SM-V [46]), as shown in Fig. 2(a). Since in realistic scenarios the coupling constant $|g| \ll 1$ (a typical value is $|g| \sim 10^{-3}$), the qubit features could be very difficult to see.

This problem can be resolved by shaped electrons, for which the interaction creates EELS features that are proportional to $|g|$ instead of to $|g|^2$. Moreover, several qubit properties remain inaccessible for unshaped electrons. One such property is T_2 . To probe T_2 , we take a superposition electron state of two (or more) different energies [Fig. 1(b)]. Such electrons lead to interference in the electron-qubit interaction, depending on the phases (in the rotating frame of reference): ϕ_g of the coupling constant, ϕ_e between the relevant electron energies (determined by the modulating laser), and ϕ_a between the excited and ground qubit states. We denote the phase difference by $\Phi = \phi_a - \phi_e - \phi_g$.

The EELS probabilities of electron energy gain P_+ and energy loss P_- depend on the phase difference Φ . Their difference $\Delta P = P_+ - P_-$, to first order in the coupling strength $|g|$, is

$$\Delta P = (P_+ + P_-)|g|e^{-\tau/T_2} \sin(\Phi). \quad (6)$$

The maximal EELS signal is for $\Phi = \pi/2 + \pi\mathbb{Z}$. The maximal contrast can be found without explicit knowledge of $\phi_{a,e}$ by scanning over different electron phases. Repeating this experiment for different τ enables measuring the decoherence time T_2 [Fig. 2(b)]. We emphasize that T_2 is the *individual* decoherence time of the given qubit, which usually cannot be measured directly (e.g., in dense ensembles). Only its average over multiple qubits can be found through collective measurement methods such as spin echo [25]. We can also use a broad electron wave function to probe many emitters simultaneously, in which case, the relevant decoherence time will be the typically much smaller collective T_2^* [25].

Equation (6) shows a remarkable quality: interference enables obtaining a net energy gain or loss proportional to $|g|$ rather than to $|g|^2$, which increases the EELS sensitivity. This quality can be exploited in multiple ways. We propose a sensitive T_1 measurement scheme in which a $\pi/2$ pulse is applied immediately before the interaction with the shaped electron. Then, we extract T_1 via a similar scheme (elaborated in SM-V [46]).

Finding the exact qubit state on the Bloch sphere.—Our method is of particular interest for setting initial conditions or measuring final states in quantum simulators. Thus far, optical tools can control individual qubits only when they are more than a wavelength apart, limiting qubit-qubit interactions and possible experimental platforms for

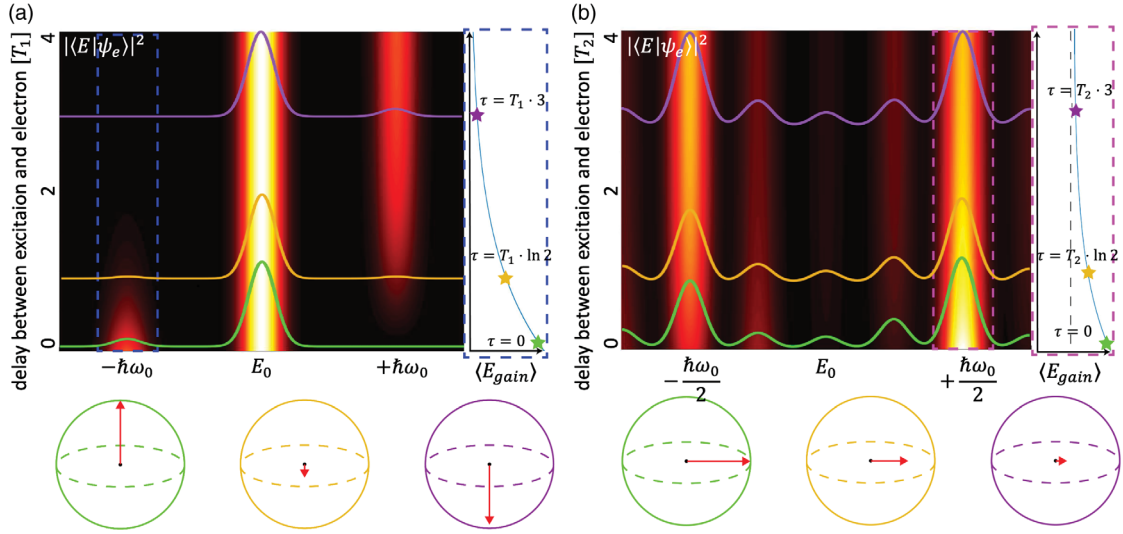


FIG. 2. Extraction of the relaxation (T_1) and decoherence (T_2) times from a sequence of delayed electron energy spectra. (a) A laser pulse excites the qubit to $|e\rangle$, which then relaxes back. T_1 is extracted from the sequence of electron energy loss spectroscopy (EELS) measurements of unshaped electrons probing the qubit at different delays τ . $\langle E_{\text{gain}} \rangle$ is the average energy gain. (b) A laser pulse excites the qubit to $1/\sqrt{2}(|g\rangle + i|e\rangle)$, which then precesses while decohering. T_2 is extracted from the sequence EELS measurements of shaped electrons probing the qubit at different delays τ .

simulators. Shaped-electron probes could enable new quantum simulator platforms, facilitated by the electrons' spatial resolution.

We present a scheme that utilizes shaped electrons [Fig. 3(a)] for measuring qubit states on the Bloch sphere. Consider a general state $|\psi_a\rangle = \cos(\theta_a/2)|e\rangle + e^{i\phi_a}\sin(\theta_a/2)|g\rangle$, with θ_a and ϕ_a representing the Bloch sphere angles. The qubit interacts with the electron $|\psi_e\rangle = |E_+\rangle + e^{i\phi_e}|E_-\rangle$ [Fig. 3(b)]. The resulting EELS probability difference $\Delta P = P_+ - P_-$, to first order in $|g\rangle$, is given by [illustrated in Fig. 3(c)]

$$\Delta P = (P_+ + P_-)|g|\sin(\theta_a)\sin(\Phi) \quad (7)$$

(elaborated in SM-V and SM-VIII [46]). The value of $\sin(\theta_a)$ can be found by repeating the measurement, scanning over ϕ_e until ΔP is maximized, $\Delta P_{\text{max}} = (P_+ + P_-)|g|\sin(\theta_a)$. To remove the ambiguity regarding whether the qubit is located on the lower or upper half of the Bloch sphere [since $\sin(\theta_a)$ is symmetric around $\theta_a = \pi/2$], one can use an additional $\pi/2$ pulse or measure additional electron spectral peaks (SM-VIII [46]).

The same scheme can extract additional information, such as the transition dipole moment size [by extracting $|g|$ from Eq. (3)], and measure the electron phase ϕ_e (by changing ϕ_a).

Probing superradiance from multiple emitters.—For qubits with weak nonradiative relaxation, T_1 is related to the qubit's spontaneous emission rate $\gamma = 1/T_1$, influenced by the optical environment through the LDOS. Thus, the shaped-electron-qubit interaction enables

measuring the LDOS through a pump-probe scheme as in Fig. 4 (more in SM-VII [46]).

This measurement scheme has a temporal resolution on femtosecond timescales [33–36,54,55], gradually reaching attosecond timescales [36,56–58]. Consequently, the scheme can be utilized to explore novel emission phenomena on short timescales, such as superradiance [Fig. 4(c)], which occurs when a few qubits are bunched together. In superradiance, several excited qubits have a faster emission rate γ than each individual qubit. Our scheme can observe the rapid decay via changes in the EELS peaks. Thus, we can quantify the superradiant decay of any number of emitters (SM-VI [46]). The superradiance implies an enhancement in CL experiments (SM-VI [46]). A different CL enhancement can be created even for a single qubit by using shaped free electrons, as discussed further in SM-V [46]. The latter corresponds to part of the predictions of a semiclassical theory [43].

Discussion and outlook.—The concepts proposed in our work can be realized in existing materials that have large dipole moments such as perovskite nanocrystals [28–30]. We estimate that temporal resolution of a hundred fs and spatial resolution reaching a single nm is achievable (SM-V [46], including Refs. [59,60]), at energy resolution limited by the excitation laser bandwidth (~ 10 meV and below [55,61]). The optimal electron velocity for a transverse dipole is $v \approx (r_\perp \omega_0/1.33)$ (SM-III [46]).

For r_\perp smaller than the dipole's size, there could be beyond-dipole corrections to the electron-qubit interaction. Then, the qubit wave function profile cannot be ignored. When the electron spot size is smaller than the qubit, as with SCQDs, we can potentially probe the qubit state and

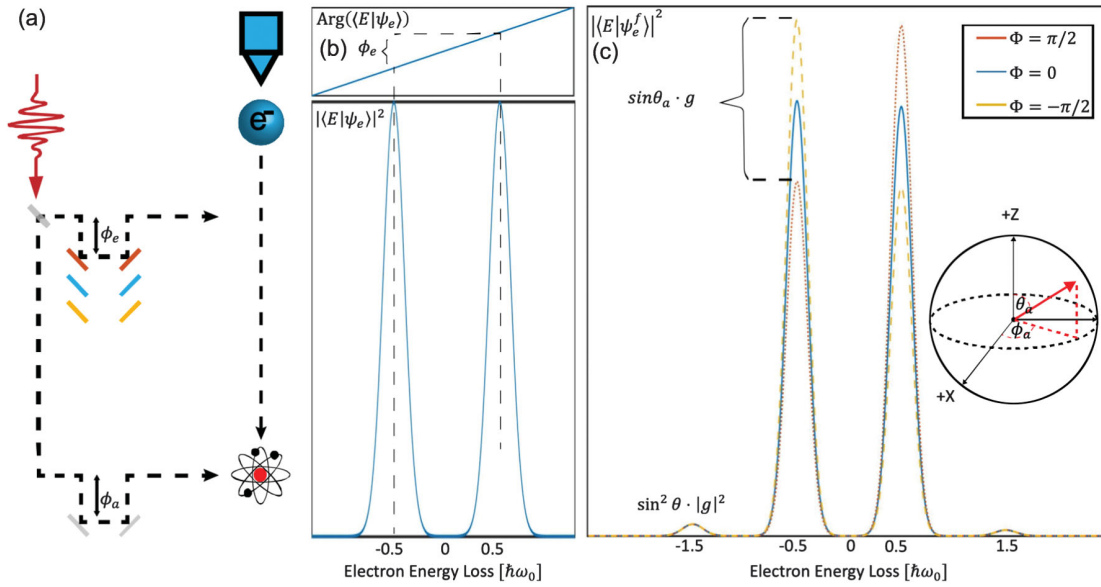


FIG. 3. A scheme for measuring the qubit state on the Bloch sphere: (a) The electron is coherently shaped by a laser pulse with a tunable optical path length that changes the relative phase ϕ_e between the electron's energy states. The same laser (or another one that is phase-locked) excites the qubit to a state defined by angles θ_a and ϕ_a on the Bloch sphere. (b) The initial electron wave function with relative phase ϕ_e . (c) The resulting EELS spectra for different ϕ_e . We extract the qubit state from the difference between the maximal and minimal EELS peaks. ϕ_g is the phase of the interaction constant g and $\Phi = \phi_a - \phi_e - \phi_g$.

decoherence time as a function of position inside a quantum dot. Such experiments can provide insight into the effects of many-body physics in quantum emitters.

The acquisition of electron spot sizes of a few nanometers opens intriguing possibilities for testing dense ensembles of qubits in systems such as SCQDs [17–19], and for measuring decoherence rates and other quantum properties of individual quantum dots in the ensemble. The

combined temporal and spatial resolution can reveal currently unobserved phenomena, such as differences in T_2 of individual qubits in the ensemble and their fluctuations in time. The electron-qubit interaction can also probe the mechanisms differentiating T_2 and T_2^* [25,26].

High-density SCQDs are of particular interest in areas of quantum technologies, being able to demonstrate fundamental coherent quantum effects such as Rabi oscillations

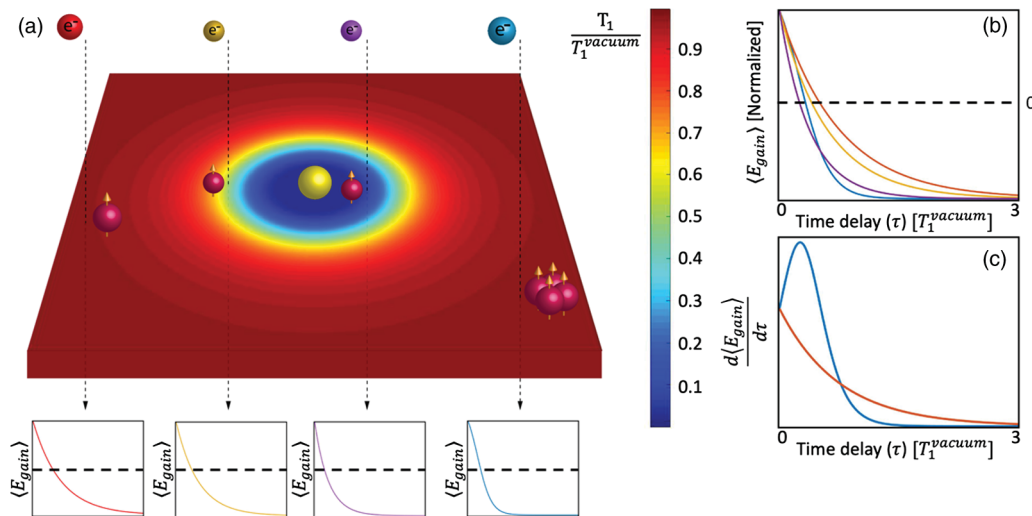


FIG. 4. Free-electron-qubit interactions for studying superradiance and mapping the local density of photonic states. (a) To exemplify the concept, we place qubits on a membrane surrounding a 10 nm Au nanoparticle, which varies the LDOS and T_1 as a function of position. (b) Comparison of the time decay of normalized $\langle E_{\text{gain}} \rangle$ for different qubit positions (the same curves are also shown schematically at the four bottom plots). (c) The emission from a single qubit (orange) vs superradiance from multiple qubits (blue).

[18,62], Ramsey fringes, photon echoes, and even quantum coherent revival [63,64]. Currently, these phenomena are probed optically, which limits researchers' ability to study the properties of single qubits out of a dense ensemble and understand how they vary within the ensemble.

We should also discuss the validity of modeling real materials with a two-level system (qubit) for interactions with free electrons. Unlike a photon that creates only a single excitation, an electron can set off many material excitations, acting as decoherence channels and becoming entangled with the electron. When the additional excitations are distinct in energy from the qubit energy, one can postselect electrons (using an energy filter) that lose or gain the qubit energy, ensuring that the measured electrons interact with the qubit. This approach is especially accurate in thin samples, where electrons only weakly interact with the decoherence channels. The resulting qubit-electron density matrix is then unchanged by these channels. Future work should further quantify the effect of general decoherence channels on our ability to infer the qubit state from the electron. Looking forward, the determination of material systems that realize the idealized interaction will be a key problem in this field.

From a different perspective, our theory can be seen as a generalization of the well-established EELS theory [65–68] for out-of-equilibrium systems that hold coherence, i.e., described by superposition of different energy states. A detailed comparison between our approach and the standard EELS theory is presented in SM-X [46]. The standard EELS theory covers a wide variety of interacting systems beyond the two-level system model here. Thus, it will be of great importance to generalize our work to create the unified theory of inelastic electron scattering (or EELS) by general time-dependent out-of-equilibrium systems.

To conclude, we predict that coherently shaped free electrons can determine the qubit state and other quantum characteristics. We envision combining this idea with the proposed methods of coherent control using shaped electrons [43,69]. Together, they constitute the building blocks to read/write the quantum state of various quantum systems using shaped electrons. Such capabilities, especially if achieved at deep subwavelength and eventually atomic resolutions, are attractive for creating new types of quantum simulators. We envision quantum simulators in which shaped electrons enable the depiction of the initial state of each element and enable reading the final (or intermediate) states using femtosecond (and ultimately attosecond [36,38,56–58]) time resolution.

We thank Prof. Gadi Eisenstein for fruitful discussions. This project has received funding from the European Union's Horizon 2020 research and innovation programme under grant agreement no. 851780-ERC-NanoEP.

Note added.—Recently, we became aware of another work [70], conducted in parallel, that partially overlaps with our

Letter. That work [70] also treated the electron-qubit interaction fully quantum mechanically, and also proposed that such interactions can enhance the electron energy gain or loss spectrum and probe the qubit coherence. Two other partially related studies [71,72] appeared in parallel with our submission, analyzing the interaction between free electrons and a two-level system, or general multilevel systems [71]. However, as these studies were motivated by other prospects, they did not discuss the idea of measuring coherent properties of the system (as in our Letter and in Ref. [70]). To measure the coherent properties, our Letter calculates interaction with systems in general superposition states (rather than the ground state [71]) and probes the coherence (off-diagonal) terms of the density matrix (rather than the qubit probabilities on the diagonal [72]).

*These authors contributed equally to this work.

†kaminer@technion.ac.il

- [1] A. Polman, M. Kociak, and F. J. G. de Abajo, Electron-beam spectroscopy for nanophotonics, *Nat. Mater.* **18**, 1158 (2019).
- [2] M. Kociak, Cathodoluminescence in the scanning transmission electron microscope, *Ultramicroscopy* **176**, 112 (2017).
- [3] M. Kuttge, Local density of states, spectrum, and far-field interference of surface plasmon polaritons probed by cathodoluminescence, *Phys. Rev. B* **79**, 113405 (2009).
- [4] F. J. G. Abajo, Probing the Photonic Local Density of States with Electron Energy Loss Spectroscopy, *Phys. Rev. Lett.* **100**, 106804 (2008).
- [5] T. Mails, S. C. Cheng, and R. F. Egerton, EELS log-ratio technique for specimen-thickness measurements in the TEM, *J. Electron Microsc. Tech.* **8**, 193 (1988).
- [6] L. Novotny, *Principles of Nano-Optics* (Cambridge University Press, New York, 2012).
- [7] M. O. Scully and M. S. Zubairy, *Quantum Optics* (Cambridge University Press, New York, 1997).
- [8] A. Bechtold, D. Rauch, F. Li, T. Simmet, P.-L. Ardel, A. Regler, K. Müller, N. A. Sinitsyn, and J. J. Finley, Three-stage decoherence dynamics of an electron spin qubit in an optically active quantum dot, *Nat. Phys.* **11**, 1005 (2015).
- [9] A. Bechtold, F. Li, K. Müller, T. Simmet, P.-L. Ardel, J. J. Finley, and N. A. Sinitsyn, Quantum Effects in Higher-Order Correlators of a Quantum-Dot Spin Qubit, *Phys. Rev. Lett.* **117**, 027402 (2016).
- [10] A. Grelich, S. G. Carter, D. Kim, A. S. Bracker, and D. Gammon, Optical control of one and two hole spins in interacting quantum dots, *Nat. Photonics* **5**, 702 (2011).
- [11] S. E. Economou and T. L. Reinecke, Theory of Fast Optical Spin Rotation in a Quantum Dot Based on Geometric Phases in Trapped States, *Phys. Rev. Lett.* **99**, 217401 (2007).
- [12] T. M. Godden, J. H. Quilter, A. J. Ramsay, Y. Wu, P. Brereton, S. J. Boyle, I. J. Luxmoore, J. Puebla-Nunez, A. M. Fox, and M. S. Skolnick, Coherent Optical Control of the Spin of a Single Hole in an InAs/GaAs Quantum Dot, *Phys. Rev. Lett.* **108**, 017402 (2012).

- [13] I. Khanonkin, A. K. Mishra, O. Karni, V. Mikhelashvili, S. Banyoudeh, F. Schnabel, V. Sichkovskiy, J. P. Reithmaier, and G. Eisenstein, Ultra-fast charge carrier dynamics across the spectrum of an optical gain media on INAs/AlGaInAs/InP quantum dots, *AIP Adv.* **7**, 035122 (2017).
- [14] N. N. Ledentsov, V. M. Ustinov, V. A. Shchukin, P. S. Kop'ev, Zh. I. Alferov, and D. Bimberg, Quantum dot heterostructures: Fabrication, properties, lasers, *Semiconductors* **32**, 343 (1998).
- [15] D. Bimber and U. W. Pohl, Quantum dots: Promises and accomplishments, *Mater. Today* **14**, 388 (2011).
- [16] H. Shen *et al.*, Visible quantum dot light-emitting diodes with simultaneous high brightness and efficiency, *Nat. Photonics* **13**, 192 (2019).
- [17] S. Banyoudeh and J. P. Reihmmer, High-density 1.54 μm InAs/InGaAlAs/InP (100) based quantum dots with reduced size inhomogeneity, *J. Cryst. Growth* **425**, 299 (2015).
- [18] H. Choi, V.-M. Gkortsas, L. Diehl, D. Bour, S. Corzine, J. Zhu, G. Höfler, F. Capasso, F. X. Kärtner, and T. B. Norris, Ultrafast Rabi flopping and coherent pulse propagation in a quantum cascade laser, *Nat. Photonics* **4**, 706 (2010).
- [19] M. Bayer and A. Forchel, Temperature dependence of the exciton homogeneous linewidth in $\text{In}_{0.60}\text{Ga}_{0.40}\text{As}/\text{GaAs}$ self-assembled quantum dots, *Phys. Rev. B* **65**, 041308 (2002).
- [20] D. Loss and D. P. DiVincenzo, Quantum computation with quantum dots, *Phys. Rev. A* **57**, 120 (1998).
- [21] M. A. Nielsen and I. Chuang. *Quantum Computation and Quantum Information* (Cambridge University Press, New York, 2002).
- [22] R. Bose, D. Sridharan, H. Kim, G. S. Solomon, and E. Waks, Low-Photon-Number Optical Switching with a Single Quantum Dot Coupled to a Photonic Crystal Cavity, *Phys. Rev. Lett.* **108**, 227402 (2012).
- [23] A. P. Alivisatos, A. L. Harris, N. J. Levinos, M. L. Steigerwald, and L. E. Brus, Electronic states of semiconductor clusters: Homogeneous and inhomogeneous broadening of the optical spectrum, *J. Chem. Phys.* **89**, 4001 (1988).
- [24] Y. Deng and D. Chu, Coherence properties of different light sources and their effect on the image sharpness and speckle of holographic displays, *Sci. Rep.* **7**, 5893 (2017).
- [25] L. Allen and J. H. Eberly. *Optical Resonance and Two-level Atoms* (Dover Publications, New York, 1987).
- [26] P. Borri, W. Langbein, S. Schneider, U. Woggon, R. Sellin, D. Ouyang, and D. Bimberg, Ultrastrong Dephasing Time in InGaAs Quantum Dots, *Phys. Rev. Lett.* **87**, 157401 (2001).
- [27] K. S. Novoselov, A. Mishchenko, A. Carvalho, and A. H. C. Neto, 2D materials and van der Waals heterostructures, *Science* **353**, aac9439 (2016).
- [28] A. K. Jena, A. Kulkarni, and T. Miyasaka, Halide perovskite photovoltaics: background, status, and future, *Chem. Rev.* **119**, 3036 (2019).
- [29] Q. A. Akkerman, G. Rainò, M. V. Kovalenko, and L. Manna, Genesis, challenges and opportunities for colloidal lead halide perovskite nanocrystals, *Nat. Mater.* **17**, 394 (2018).
- [30] B. R. Sutherland and E. H. Sargent, Perovskite photonic sources, *Nat. Photonics* **10**, 295 (2016).
- [31] R. G. Hulet, E. S. Hilfer, and D. Kleppner, Inhibited Spontaneous Emission by a Rydberg Atom, *Phys. Rev. Lett.* **55**, 2137 (1985).
- [32] R. R. Jones, D. You, and H. B. Bucksbaum, Ionization of Rydberg Atoms by Subpicosecond Half-Cycle Electromagnetic Pulses, *Phys. Rev. Lett.* **70**, 1236 (1993).
- [33] B. Barwick, D. J. Flannigan, and A. H. Zewail, Photon-induced near-field electron microscopy, *Nature (London)* **462**, 902 (2009).
- [34] S. T. Park, M. Lin, and A. H. Zewail, Photon-induced nearfield electron microscopy (PINEM): Theoretical and experimental, *New J. Phys.* **12**, 123028 (2010).
- [35] A. Feist, K. E. Echternkamp, J. Schauss, S. V. Yalunin, S. Schäfer, and C. Ropers, Quantum coherent optical phase modulation in an ultrafast transmission electron microscope. *Nature (London)* **521**, 200 (2015).
- [36] K. E. Priebe, C. Rathje, S. V. Yalunin, T. Hohage, A. Feist, S. Schäfer, and C. Ropers, Attosecond electron pulse trains and quantum state reconstruction in ultrafast transmission electron microscopy, *Nat. Photonics* **11**, 793 (2017).
- [37] G. M. Vanacore *et al.*, Ultrafast generation and control of an electron vortex beam via chiral plasmonic near fields. *Nat. Mater.* **18**, 573 (2019).
- [38] G. M. Vanacore *et al.*, Attosecond coherent control of free-electron wave functions using semi-infinite light fields, *Nat. Commun.* **9**, 2694 (2018).
- [39] K. E. Echternkamp, A. Feist, S. Schäfer, and C. Ropers, Ramsey-type phase control of free-electron beams. *Nat. Phys.* **12**, 1000 (2016).
- [40] O. Kfir, Entanglements of Electrons and Cavity Photons in the Strong-Coupling Regime, *Phys. Rev. Lett.* **123**, 103602 (2019).
- [41] V. D. Giulio, M. Kociak, and F. J. G. Abajo, Probing quantum optical excitations with fast electrons, *Optica* **6**, 1524 (2019).
- [42] Y. Pan and A. Gover, Spontaneous and stimulated emission of a preformed quantum free-electron wave function, *Phys. Rev. A* **99**, 052107 (2019).
- [43] A. Gover and A. Yariv, Free-Electron-Bound-Electron Resonant Interaction, *Phys. Rev. Lett.* **124**, 064801 (2020).
- [44] R. H. Dicke, Coherence in spontaneous radiation processes, *Phys. Rev.* **93**, 99 (1954).
- [45] M. Gross and S. Haroche, Superradiance: An essay on the theory of collective spontaneous emission, *Phys. Rep.* **93**, 301 (1982).
- [46] See Supplemental Material at <http://link.aps.org/supplemental/10.1103/PhysRevLett.126.233403> which contains X sections that expand on the theory and concept presented in the Letter.
- [47] M. E. Peskin and D. V. Schroeder, *An Introduction to Quantum Field Theory* (CRC Press, Reading, 2018).
- [48] D. B. Williams and C. B. Carter, *Transmission Electron Microscopy* (Springer, Boston, 2009).
- [49] J. D. Jackson, *Classical Electrodynamics* (Wiley, New York, 1999).
- [50] V. Baryshevsky *et al.*, *Parametric X-Ray Radiation in Crystals* (Springer, Berlin, 2005).
- [51] W. Magnus, On the exponential solution of differential equations for a linear operator, *Commun. Pure Appl. Math.* **7**, 649 (1954).
- [52] N. Rivera and I. Kaminer, Light-matter interactions with photonic quasiparticles, *Nat. Rev. Phys.* **2**, 538 (2020).

- [53] H.-P. Breuer, *The Theory of Open Quantum Systems* (Oxford University Press, New York, 2002).
- [54] R. Dahan *et al.*, Resonant phase-matching between a light wave and a free-electron wavefunction, *Nat. Phys.* **16**, 1123 (2020).
- [55] K. Wang, R. Dahan, M. Shentcis, Y. Kauffmann, A. B. Hayun, O. Reinhardt, S. Tsesses, and I. Kaminer, Coherent interaction between free electrons and a photonic cavity, *Nature (London) Phys. Sci.* **582**, 50 (2020).
- [56] Y. Morimoto and P. Baum, Diffraction and microscopy with attosecond electron pulse trains, *Nat. Phys.* **14**, 252 (2018).
- [57] M. Kozák, N. Schönenberger, and P. Hommelhoff, Ponderomotive Generation and Detection of Attosecond Free-Electron Pulse Trains, *Phys. Rev. Lett.* **120**, 103203 (2018).
- [58] O. Reinhardt and I. Kaminer, Theory of Shaping Electron Wavepackets with Light, *ACS Photonics* **7**, 2859 (2020).
- [59] D. C. Bell and N. Erdman, *Low Voltage Electron Microscopy: Principles and Applications* (Wiley, New York, 2012).
- [60] G. Bracco and B. Holst, *Surface Science Techniques* (Springer, Berlin, 2013).
- [61] E. Pomarico, I. Madan, G. Berruto, G. M. Vanacore, K. Wang, I. Kaminer, F. J. G. de Abajo, and F. Carbone, meV resolution in laser-assisted energy-filtered transmission electron microscopy, *ACS Photonics* **5**, 759 (2018).
- [62] O. Karni, A. Capua, G. Eisenstein, V. Sichkovskiy, V. Ivanov, and J. P. Reithmaier, Rabi oscillations and self-induced transparency in InAs/InP quantum dot semiconductor optical amplifier operating at room temperature, *Opt. Express* **21**, 26786 (2013).
- [63] I. Khanonkin, A. K. Mishra, O. Karni, S. Banyoudeh, F. Schnabel, V. Sichkovskiy, V. Mikhelashvili, J. P. Reithmaier, and G. Eisenstein, Ramsey fringes in room-temperature quantum-dot semiconductor optical amplifier, *Phys. Rev. B* **97**, 241117 (2018).
- [64] I. Khanonkin *et al.*, Room temperature quantum coherent revival in an ensemble of artificial atoms, [arXiv:2010.15198](https://arxiv.org/abs/2010.15198).
- [65] F. J. G. Abajo, Optical excitations in electron microscopy, *Rev. Mod. Phys.* **82**, 209 (2010).
- [66] V. U. Nazarov, Multipole surface-plasmon-excitation enhancement in metals, *Phys. Rev. B* **59**, 9866 (1999).
- [67] V. U. Nazarov, V. M. Silkin, and E. E. Krasovskii, Role of the kinematics of probing electrons in electron energy-loss spectroscopy of solid surfaces, *Phys. Rev. B* **93**, 035403 (2016).
- [68] V. U. Nazarov, V. M. Silkin, and E. E. Krasovskii, Probing mesoscopic crystals with electrons: One-step simultaneous inelastic and elastic scattering theory, *Phys. Rev. B* **96**, 235414 (2017).
- [69] D. Ratzel *et al.*, A quantum klystron: Controlling quantum systems with modulated electron beams, [arXiv:2004.10168](https://arxiv.org/abs/2004.10168).
- [70] Z. Zhao, X.-Q. Sun, and S. Fan, preceding Letter, Quantum Entanglement and Modulation Enhancement of Free-Electron-Bound-Electron Interaction, *Phys. Rev. Lett.* **126**, 233402 (2021).
- [71] F. J. G. Abajo and V. D. Giulio, Quantum and classical effects in sample excitations by electron beams, [arXiv:2010.13510](https://arxiv.org/abs/2010.13510).
- [72] A. Gover *et al.*, Resonant interaction of modulation-correlated quantum electron wavepackets with bound electron states, [arXiv:2010.15756](https://arxiv.org/abs/2010.15756).